ELSEVIER

Journal of Alloys and Compounds 330–332 (2002) 342–347

Journal of ALLOYS AND COMPOUNDS

www.elsevier.com/locate/jallcom

In situ monitoring of optical and structural switching in epitaxial YH_x switchable mirrors

J.W.J. Kerssemakers*, S.J. van der Molen, R. Günther, B. Dam, R. Griessen

Division of Physics and Astronomy, Faculty of Sciences, Vrije Universiteit, De Boelelaan 1081, NL-1081 HV Amsterdam, The Netherlands

Abstract

A detailed study is presented of the spectacular 'Manhattan switching', occurring during hydriding of epitaxial YH_x switchable mirrors. Manhattan switching involves block-wise domain switching, both in an optical and a structural sense, of discrete areas of a switchable mirror between its conductive metallic YH_2 state and its insulating YH_3 state. By means of in situ atomic force microscopy we link this domain-wise switching to the accompanying changes in resistivity and transmission of a switching mirror. We find that, relative to the optical transition and the resistivity, the structural switching is retarded compared to polycrystalline films. Further, the Manhattan effect is governed by the switching properties of the domain boundaries, that form a regular, connected network of ridges. This crucial role of the network can well be explained by assuming local variations of mechanical properties around each ridge. The findings stress the importance of local investigations on switchable mirrors.

Keywords: Hydrogen in metals; Vapour deposition; Atomic force microscopy; Metal–insulator transitions; Surface analysis

1. Introduction

Near their hydrogen induced metal–insulator transition, rare earth films, *switchable mirrors,* exhibit spectacular optical changes [1,2]. Recently, the occurrence of equally spectacular *structural* changes, the 'Manhattan effect', was discovered in *epitaxial* switchable mirrors [3]. In these films, the mirror surface is divided in micrometer sized domains, bound by a permanent triangular ridge network as shown in Fig. 1. It is formed during the first loading [3,4], when the film expands in-plane in the metallic α ($YH_{x<0.20}$) phase and during the α–β transition ($YH_{x<0.20}$–$YH_{1.9}$) [5]. Alter this first loading, no additional ridges are created. Upon both hydrogen loading and unloading between the higher concentration phases β ($YH_{1.9-2.1}$) and γ ($YH_{2.1<x<3-\delta}$) each of the enclosed domains switches at an individual rate, independent of its neighbours. Within each domain, a uniform hydrogen concentration is attained, while between adjacent domains *lateral* hydrogen transport [6] is blocked. The result is a spectacular discretization of optical switching in optically visible triangular domains. Similarly, large structural changes proceed domain-wise, leading to a dynamic 'Manhattan skyline' of expanding and contracting domains (see also Fig. 2). Manhattan switching is a nice example of the complex interplay between hydrogen concentration, stress and structural changes in switchable mirrors. The effect is not observed on the optically homogeneous polycrystalline mirrors [2,7].

Underlying the Manhattan effect are the structural transitions from the yttrium lattice during hydrogenation. When the hydrogen concentration x=[H]/[Y] increases from 0 to 3, the symmetry of the Y lattice changes from the hcp-α phase via fcc-β to the hexagonal-γ phase [8–10]. In doing so, the film expands 4.5 and 9.3% respectively along the hexagonal axis, which is the [111] direction in fcc-β and the [0001] direction in hex-γ. Such structural changes are most prominently visible in the local topography of *epitaxial* switchable mirrors [3–5,11], where these hexagonal planes are stacked parallel to the substrate both in the fcc and the hexagonal phase. Given the large lattice expansion at the phase transition, the films are remarkably robust and allow for many cycles of switching without any observable degradation [4].

So far, Manhattan switching was only investigated qualitatively, probing the surface of a mirror with an atomic force microscope (AFM) during hydrogen (un)loading. The link between optical and structural patterns was established by comparing an AFM image of films with very slow switching kinetics with the transmission image of the same surface area, as measured by an optical

*Corresponding author. Tel.: +31-20-444-7912.

E-mail address: kers@amolf.nl (J.W.J. Kerssemakers).

0925-8388/02/$ – see front matter
PII: S0925-8388(01)01441-4

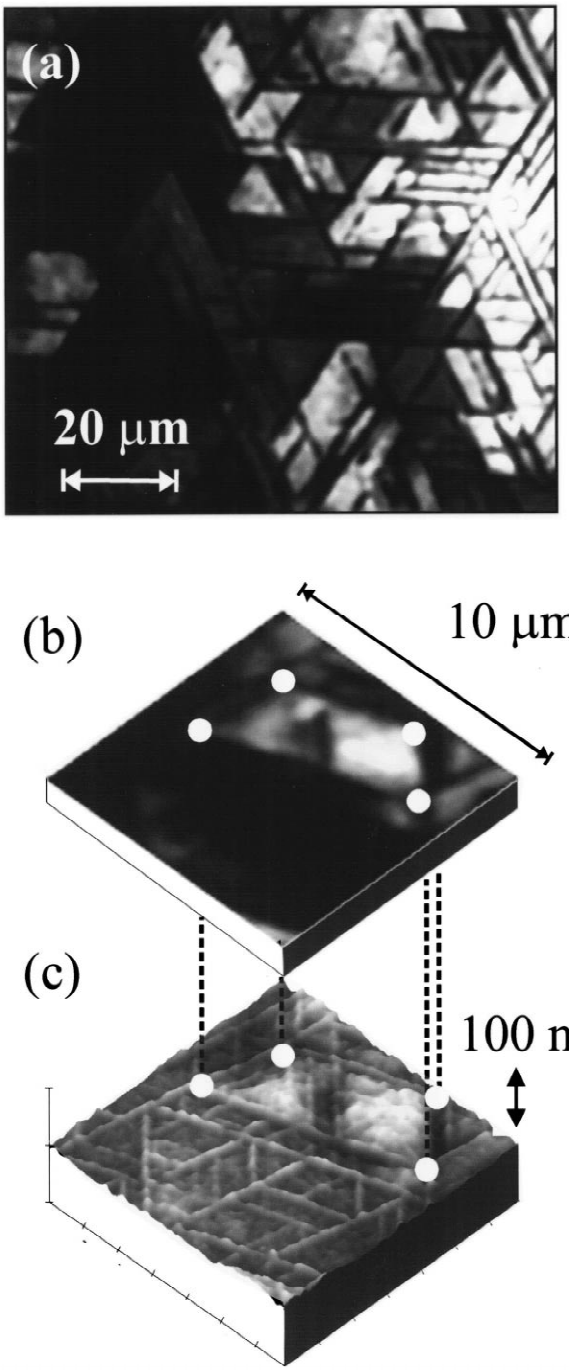

Fig. 1. Manhattan switching. (a) Optical transmission image of a 400 nm thick epitaxial YH_x film, capped by 5 nm of Pd and 25 nm of CaF_2. Visible is a triangular network of dark ridges, bounding domains which are either transparent $YH_{3-\delta}$ or dark YH_2. (b+c) A correlated, high–low pattern occurs in the topography of the surface (see also Fig. 3) when the same area is imaged by atomic force microscopy. A triangular network of protruding ridges surrounds domains which are either low or high, implying that a relation exists between local film transparency and local relative height.

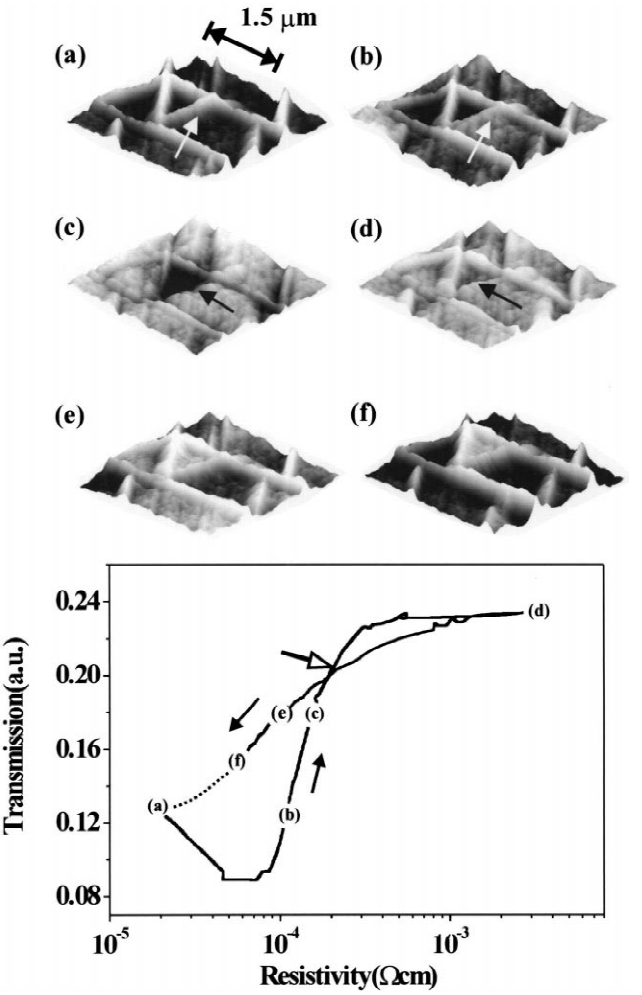

Fig. 2. Cyclic structural changes during the second hydriding cycle of a 350 nm thick epitaxial Y film capped by 5 nm of Pd; measured during in situ hydrogenation in an atomic force microscope (AFM) and a simultaneous transmission vs. resistivity measurement. (a–d): Stages in surface structure changes during loading and unloading. Corresponding points in the plot are marked. (a) fcc-β Dihydride surface showing a ridge network enclosing domains. (b) Expansion of some domains is recognizable by a relative lowering of the ridges (for example at the white arrows), indicating the onset of the fcc-β to the (expanded) hex-γ phase transition. (c) Nearly completely expanded hex-γ surface, except for one (lowered) fcc-β domain (black arrow). Ridges are almost fully immersed in the swollen domains. (d) Trihydride surface. The last domain has also switched to hex-γ. In (d) the ridges protrude more than in (c), indicating separate ridge switching. All ridges switch in a narrow region marked by the open arrow in the plot. (e, f) Upon unloading, an *inversion* of domain height can be seen when (c) and (f) are compared. This indicates a relative slow switching of the marked triangle in *both* directions. The dashed line indicates the film behavior for full unloading to its initial dihydride state.

microscope (Fig. 1). Following such an approach, it remained unclear how the structural patterns related to the average optical transmission and the overall resistivity of the mirror. These two properties are frequently used as reference parameters [1,9] as they both change continuously as a function of hydrogen concentration [10].

In the present work, we establish this link by measuring both resistivity and transmission during AFM measurements of a mirror, while it is simultaneously loaded or unloaded with hydrogen. The resistivity applies to the

whole sample surface, while the transmission is measured in an area of approximately 40×40 μm^2 around the AFM tip. In general, on such an area the transmission is representative for the average transmission of the whole sample [12]. We show that the structural changes of an epitaxial YH_x-film can be perfectly monitored by AFM. As will be shown elsewhere [12], any *relative* height change as measured by AFM corresponds to a proportional change of the relative amount of fcc dihydride phase and the hexagonal phase beneath the AFM tip [4,8,10], allowing for quantitative analysis. The great advantage of AFM is to yield detailed spatial information, in contrast to bulk techniques such as X-ray diffraction [4,10,13]. In literature, most conclusions are based on the average behavior of a thin film. Here, we show that the loading of *epitaxial* films can only be understood from local measurements.

2. Experimental

Epitaxial yttrium films are prepared by ultra high vacuum deposition (10^{-9} mbar) at substrate temperatures of 400–700°C on (111) CaF_2. A thin Pd layer is put on top, as this is necessary to dissociate H_2 to atomic H during hydrogenation. Prior to this Pd deposition, dry oxidation of the Y surface at 10^{-5} mbar for 25 min prevents the diffusion of Pd into yttrium [7,14]. For the comparative measurements as shown in Fig. 1, a thick (25 nm) buffer layer of CaF_2 was added between the Pd and the Y, slowing down the film kinetics considerably.

The Nanoscope III Tapping Mode/Contact Mode AFM is equipped with a standard 'fluid cell'. In the cell, a sample is hydrogenated in a continuously flowing mixture of H_2 and ambient air [12] at room temperature. The optical transmission is measured using the built-in laser of the AFM and a photodiode on the back of the sample. This is possible since a fraction of the focused laser beam also irradiates the sample surface around the tip. The overall resistivity is measured in a four-point configuration [15], with four contact pads evenly distributed on the outer rim of the sample and fixed with silver paste.

We use transmission vs. resistivity curves when we interpret the observed topography changes as measured with the AFM. This is possible since both resistivity and transmission changes are continuous functions of hydrogen concentration: each data point [resistivity, transmission] represents a unique hydrogenation state of a switching mirror.

3. Results

Using the in situ AFM setup, a 350 nm thick epitaxial YH_x film was loaded and unloaded several times at room temperature. In Fig. 2, the transmission vs. resistivity plot of the second loading–unloading cycle is shown, as the first loading cycle is less characteristic for the reversible Manhattan switching due to transient effects. The plot exhibits strong hysteresis, an effect described earlier by Kooij [10] on polycrystalline films. During acquisition of the resistivity and the transmission data, the surface was imaged continuously with the AFM, some representative examples of which are shown in Figs. 2(a–f). The actual scanned area is of the same order of magnitude as that from which the transmission is measured. Fig. 2(a) corresponds to the lowest possible H-concentration in the cyclic process, i.e. $x\approx1.9$. A triangular ridge network can be observed. When the film is exposed to hydrogen, the transmission decreases towards the local optical minimum at a hydrogen concentration $x=2.1$ [10]. Just after this minimum, domains start rising. This can be recognized in Fig. 2(b) as a relative *lowering* of the ridges, which are inactive in this stage of hydrogenation (for example at the white arrows). The domain rising indicates a change from (low) fcc β phase to (high) hexagonal γ phase per domain, as such significant lattice expansions as a function of hydrogen loading only occur for the phase transition, and not within each phase [8,10]. No structural changes are observed before the film has the minimal optical transmission. This is very different from polycrystalline films, for which in situ X-ray diffraction indicates that the fcc to hexagonal transition *ends* at the transmission minimum [10].

In the state corresponding to Fig. 2(c), almost all domains have fully switched to γ, leaving only one lowered fcc β domain (marked by the black arrow). During subsequent loading to γ-$YH_{3-\delta}$, this last domain eventually also switches, as can be seen in Fig. 2(d).

During the rising of the domains, the ridge pattern stays unchanged up to the state corresponding to Fig. 2(c). Compared with the initial state shown in 2(a), the ridges are almost immersed in the fully expanded domains. However, immediately after the last domains have reached full expansion, the ridges suddenly start to protrude again. This indicates *ridge switching*, occurring within a very narrow range of overall resistivity and transmission, at the point marked by the open arrow in the plot.

Upon unloading, which is performed by flowing the cell with air only, a remarkably different behavior occurs: domains which switch relatively late from fcc-β to hexagonal-γ (like the triangle in Fig. 2(c) and 2(d)) are also retarded in switching back from γ to β, during unloading, see Fig. 2(e) and 2(f). For full cycles between $YH_{1.9}$ and γ-$YH_{3-\delta}$, this results in an *inversion* of the domain height distribution, which is clearly visible when (c) and (f) are compared. This implies that the kinetics of some domains are relatively slow during both loading and unloading. As for the ridges, which showed a distinct and collective structural transition during loading, no such sharp change is observed during unloading. Still, the ridges should switch back to fcc β,as the observed transition during loading occurs every time the film is re-loaded. For

continued unloading, the film returns in its dihydride state, both for transmission and resistivity (dashed line in graph) as for the topography, as in (a).

The phase growth in the domains and the local orientation of the ridges are related. This is shown in a experiment shown in Fig. 3(a), where the AFM profile of a single ridge is followed in time as a 400 nm YH_2 film is slowly loaded to $YH_{3-\delta}$. Ridges have a regular, *asymmetric* cross section (see Fig. 3b), originating from the in-plane stresses occurring before and during the α–β transition [3,4]. In the evolution of the profiles in Fig. 3(a), taken at 100 s time intervals, it can clearly be observed that the expanded γ phase grows from the shallow face of the ridge into a domain, here from the ridge to the left. The last part of the domain surface to rise is that adjacent to the steep side of a ridge, as can be observed clearly at an intermediate profile (solid dots). Such asymmetric phase growth is seen on all ridges, irrespective of the local geometry of the ridge pattern. The cumulative rise amounts to ~40% of the film thickness, which nicely corresponds to the expected β–γ *c*-axis expansion (9.3%). We note that the steepest ridge angles are well below 10° and the AFM scan rate was only 1 scanline per 0.25 s, so that tip effects (tip convolution and sweeping) can be excluded.

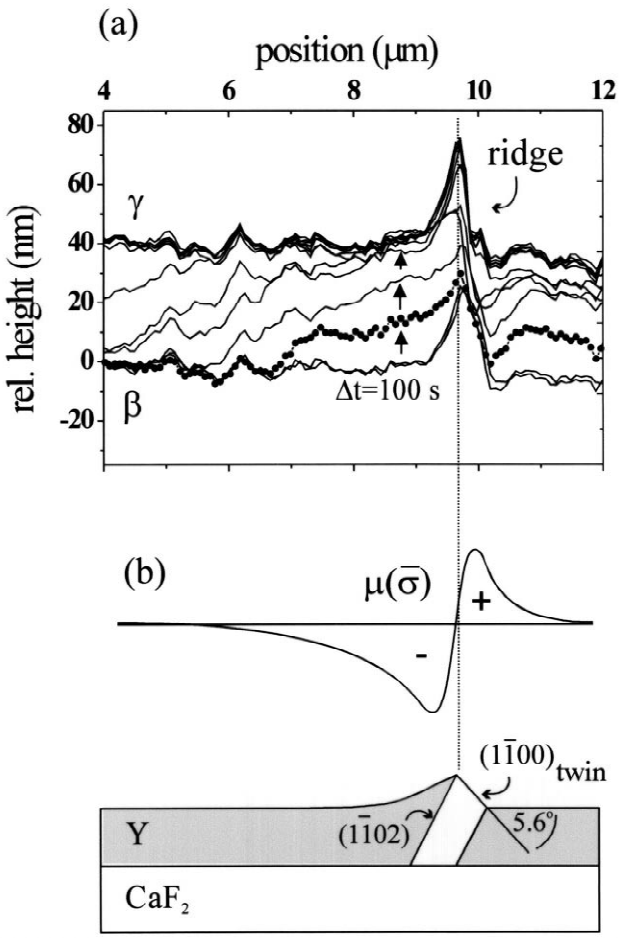

Fig. 3. Hexagonal γ-phase growth. (a), In situ AFM line profiles around an 400 nm YH_2 film during the transition of the fcc to the expanded hex-γ phase. Profiles are taken at 100 s time intervals. Expansion starts on the left side of the ridge, while the right (steepest) side expands later than the domain surface. (b) Schematic concept of expansion-induced chemical stress potential (for loading) around a ridge, linked to the asymmetric structure of a ridge. Such a potential gradient could be caused by relatively hard (steep) and soft (shallow) sides of a ridge, originating from the deformation processes which generated them during the first loading cycle. The hydrogen distribution will oppose such a potential, as can be seen clearly at an intermediate profile, shown as solid dots in (a).

The inhibited phase growth, here on the right side of the ridge, should not be confused with ridge switching itself while the domains are rising at widely varying times, the ridges are 'waiting for each other', i.e. even ridges which are relatively early surrounded by fully expanded domains, do not switch earlier than other ridges.

Summarizing, we observe two distinct structural changes on the surface of a switching epitaxial mirror, both involving the β–γ phase transition. First, the switching of the domains, which starts in the global transmission minimum, i.e. at a concentration $x=2.1$ [10], and proceeds over a large concentration range afterwards. Second, the structural switching of the ridges. The switching of domains and ridges differs remarkably: while the domains switch at widely varying individual rates, during a large change of overall resistivity and average transmission (see the plot in Fig. 2), the ridges switch almost collectively, with hardly any change in resistivity or transmission. This is noteworthy, as the fraction of the film consisting of ridge material is approximately 25% and thus by no means negligible.

Furthermore, we observe a ranking in switching times: switching is fastest (i.e. earliest) on the shallow side of a ridge. Next, the flat areas of the domains start expanding. The last part of the surface of the domains to rise is that closely adjacent to the steep side of a ridge. Finally, only after all domains have fully expanded, the ridges themselves rise to their final elevation.

4. Discussion

The ridge properties were already noted as an important factor in Manhattan switching [3]. Now, we observed that the ridges also play a role in the initial growth of the γ phase in the fcc-β domains, with a distinct ranking of switching times of the various parts of the film surface. A qualitative understanding of this ranking follows from the local chemical potential, which in a simplified, isotropic form can be written as $\mu = \sigma V + \mu_H$, where σ is a local, position dependent hydrostatic stress, V is the atomic volume per H and μ_H depends on hydrogen concentration only. As the β–γ phase transition involves a fixed volumetric expansion (or contraction) of 10%, it is convenient to write σ in terms of strain ε: $KV\varepsilon + \mu_H$, where K is an appropriate compression modulus. As long as the sample surface is in contact with the hydrogen flow, μ should be

constant, implying that the local hydrogen concentration, which governs μ_H, varies opposite to any local stress σ. As a consequence, a new phase is likely to initiate on 'soft' (low K) spots, whether it involves an expansion (for loading) or a contraction (for unloading). Based on observations as in Figs. 2 and 3, we now assume that a ridge has a 'soft' (low K) shallow side and a 'hard' (high K) steep side. This is not unlikely, as the ridges originate from a plastic, deformative process [3,4]. Thus, we can define a 'potential landscape' linked to the ridge pattern (see Fig. 3b), with for each ridge, a relatively unfavorable 'hard' side for hydrogen to enter, and a relatively favorable 'soft' side. The concept also nicely explains the twofold functioning of a ridge as a barrier for lateral hydrogen transport (due to the hard side) and as a mechanical decoupler for the switching domains (due to the soft side) [3].

We can now understand the wide variation in domain switching from a simple geometrical argument, as shown schematically in Fig. 4. The ridge network is regular [3] but the orientation of a single ridge, i.e. the direction of the hard, phase growth inhibiting side, is random. Because the ridge network is fully connected, statistically there will be domains which are surrounded by hard sides of ridges only, as schematized in Fig. 4b. In this view, we expect the slowest domains to be small triangles fully surrounded by steep sides, as they will be most strongly inhibited in the phase transition in *both* directions ($\beta \rightarrow \gamma$ and $\gamma \rightarrow \beta$). This is exactly what is observed in practice, see for example Fig. 2(c) and (f): the retarded small domain is confined between three steep sides. As this reasoning naturally does not hold for the ridges themselves, we can also now understand why the ridges switch much more collectively than the domains.

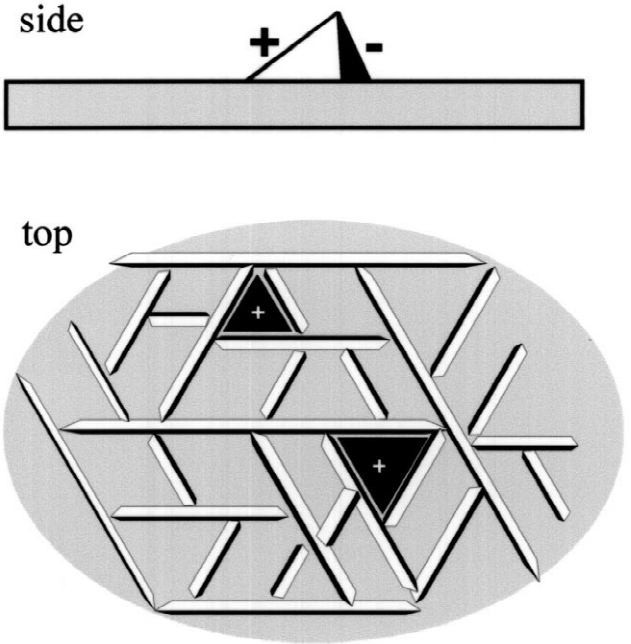

Fig. 4. The random distribution of interconnected ridges leads to a fraction of domains that are bounded only by steep, phase growth inhibiting sides (marked '+'). Such domains tend to exhibit retarded switching, for both the $\beta \rightarrow \gamma$ transition during loading and the $\gamma \rightarrow \beta$ transition during unloading. An example of such a relatively slow switching domain is visible in Fig. 2(c) and 2(f).

5. Conclusions

By continuous, in situ monitoring with AFM of the Manhattan switching on hydriding epitaxial YH_x mirrors, we found a qualitative difference with polycrystalline films. For epitaxial films, the transition of the fcc-β to hexagonal-γ phase starts after the optical transmission minimum is reached, while for polycrystalline films this minimum marks the end point of the β–γ transition. Furthermore, we find that the connected ridge network present on epitaxial films plays a crucial role in structural switching. Apart from being mechanical decouplers and hydrogen barriers, the ridges also directly influence the switching of the domains: phase growth starts on one ridge side only. Due to differences in the local geometry of the ridges, this leads to large differences in local switching rates of the domains. All observations can be understood by assuming the ridges have asymmetrical mechanical properties. The ridges themselves switch almost collectively after the domains during loading. In essence, an epitaxial YH_x mirror consists of two switching components, domains and ridges, with very different kinetics. This finding stresses the importance of microscopic investigations of switchable mirrors.

Acknowledgements

This work was supported by the Stichting voor Fundamenteel Onderzoek der Materie (FOM), which is financed by N.W.O. We also acknowledge financial contribution of the European Commission through the TMR program (research network 'Metal hydrides with switchable physical properties').

References

[1] J.N. Huiberts, R. Griessen, J.H. Rector, R.A. Wijngaarden, J.P. Dekker, D.G. de Groot, N.J. Koeman, Nature 380 (1996) 231.
[2] M. Kremers, N.J. Koeman, R. Griessen, P.H.L. Notten, R. Tolboom, P.J. Kelly, P.A. Duine, Phys. Rev. B 57 (1998) 4943.
[3] J.W.J. Kerssemakers, S.J. van der Molen, N.J. Koeman, R. Gunther, R. Griessen, Nature (London) 406 (2000) 489.
[4] D.G. Nagengast, J.W.J. Kerssemakers, A.T.M. van Gogh, B. Dam, R. Griessen, Appl. Phys. Lett. 75 (1999) 1724.
[5] E.J. Grier, O. Kolosov, A.K. Petford-Long, R.C.C. Ward, M. R Wells, B. Hjörvarsson, J Phys. D: Appl. Phys. 33 (2000) 894.
[6] F.J.A. den Broeder, S.J. van der Molen, M. Kremers, J.N. Huiberts,

D.G. Nagengast, A.T.M. van Gogh, W.H. Huisman, N.J. Koeman, B. Dam, J.H. Rector, S. Plota, M. Haaksma, R.M.N. Hanzen, R.M. Jungblut, P.A. Duine, R. Griessen, Nature 394 (1998) 656.
[7] S.J. van der Molen, J.W.J. Kerssemakers, J.H. Rector, N.J. Koeman, B. Dam, R. Griessen, J. Appl. Phys. 86 (1999) 6107.
[8] Chapter 20 P. Vajda, in: K.A. Gschneider, L. Eyring (Eds.), Handbook on the Physics and Chemistry of Rare Earths, Elsevier, Amsterdam, 1995, pp. 207–291.
[9] A.T.M. van Gogh, D.G. Nagengast, E.S. Kooij, N.J. Koeman, R. Griessen, Phys. Rev. Lett. 85 (2000) 2156.
[10] E.S. Kooij, A.T.M. van Gogh, D.G. Nagengast, N.J. Koeman, R. Griessen, Phys. Rev. B 62 (2000) 10088.
[11] A. Pundt, M. Getzlaff, M. Bode, R. Kirchheim, R. Wiesendanger, Phys. Rev. B 61 (15) (2000) 9964.
[12] Kerssemakers et al., to be published.
[13] A. Remhof, G. Song, Ch. Sutter, A. Schreyer, R. Siebrecht, H. Zabel, F.G. Thoff, J. Windgasse, Phys. Rev. B 59 (1999) 6689.
[14] A.T.M. van Gogh, S.J. van der Molen, J.W.J. Kerssemakers, N.J. Koeman, R. Griessen, Appl. Phys. Lett. 77 (2000) 815.
[15] L.J. van der Pauw, Philips Res. Repts. 13 (1958) 1.